Journal of Catalysis **183,** 210–221 (1999)
Article ID jcat.1999.2397, available online at http://www.idealibrary.com on IDEAL®

Kinetic Study of the Oxidative Dehydrogenation of Butane on V/MgO Catalysts

C. Téllez, M. Menéndez,[1] and J. Santamaría

Department of Chemical and Environmental Engineering, University of Zaragoza, 50009 Zaragoza, Spain

Received July 1, 1998; revised December 24, 1998; accepted December 26, 1998

A kinetic study of the oxidative dehydrogenation of butane over V/MgO catalysts has been carried out. The rate equations for the oxidation of each of the hydrocarbons in the proposed reaction network were obtained independently, and specific experiments were also performed to evaluate inhibition effects of the reaction products on the butane reaction rate. Several competing kinetic models were statistically analyzed. The best fit was obtained with a dual-site Mars–van Krevelen model, the suitability of which was also tested in separate anaerobic experiments. Furthermore, this model was able to predict reactor performance under conditions far removed from those employed in the differential reactor experiments used to obtain the kinetics. © 1999 Academic Press

Key Words: **reaction kinetics; reaction mechanism; oxidative dehydrogenation; butane; V/MgO catalysts.**

1. INTRODUCTION

A widely studied alternative for the production of olefins is the oxidative dehydrogenation (ODH) of paraffins. This process offers the possibility of avoiding or minimizing several of the problems encountered in classic dehydrogenation: (a) the conversion is limited by the thermodynamic equilibrium, (b) heat must be supplied at high temperature, due to the endothermic nature of the reaction, (c) the catalyst is deactivated by coke formation, and (d) large amounts of by-products are obtained due to cracking reactions. ODH has been studied for feedstocks ranging from ethane to pentane, and the results have been described in several reviews (1–3). This work is concerned with the oxidative dehydrogenation of butane, yielding butane and butadiene as the desired products. Among other uses, butadiene production by ODH of butane has been recently proposed as a potential new route for styrene production (4). The main problem associated with the oxidative dehydrogenation of alkanes is the simultaneous formation of carbon oxides by the nonselective oxidation of hydrocarbon reactants and products. Many catalyst formulations, such as metallic ferrites, supported vanadium oxides, vanadates, metal molybdates and nickel-based systems, have been tested in an attempt to increase the selectivity of butane ODH (3). Among the more promising materials, V–Mg–O catalysts have shown high yields and stable operation (5–7).

As in many other oxidation reactions, the kind of reactor employed strongly influences the attainable yield (8, 9). To design and optimize the most suitable reactor a kinetic model is required that describes closely the behavior of the system under a variety of conditions. The first study on the kinetics of butane ODH over a V/MgO catalyst was carried out by Chaar *et al*. (5), who proposed the following reaction scheme:

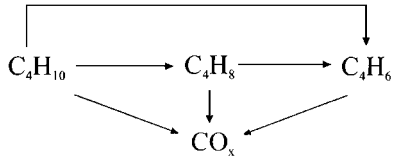

[1]

These authors employed simple power-law kinetics, with zero apparent order for oxygen and 0.85 for the hydrocarbon in all the reactions. A later study (10) confirmed butadiene as both a primary and a secondary product of the reaction. The kinetics of butane ODH has also been studied over several other catalysts, such as Ni–V–Sb (11), Cs–Ni–Mo (12), and V–Mg–Al (13). All of these catalysts gave a lower selectivity at a given conversion compared with the V/MgO catalyst. It therefore seems worthwhile to study with more detail the kinetics of butane ODH over V/MgO.

Several mechanisms have been proposed for this reaction, leading to Langmuir–Hinshelwood (13)- or Mars–van Krevelen (12)-type kinetics. Sometimes inhibition by CO_2 has been reported (11). A similar reaction, the ODH of propane, has also been the subject of a number of studies. Anderson (14) proposed an Eley–Rideal mechanism for $V/AlPO_4$, whereas a Mars–van Krevelen mechanism gave

[1] To whom correspondence should be addressed. Fax: +34976 762142. E-mail: IQCATAL@POSTA.UNIZAR.ES.

0021-9517/99 $30.00

the best fit of experimental data obtained over V–Sb–Mg (15), Ni–Co/Al_2O_3 (16), and V/MgO (17–19). In some cases (2, 18, 19), different levels for the degree of oxidation of the active sites were postulated.

In view of the discrepancies encountered in previous studies, the objective of this work is to obtain an improved kinetic model for butane ODH on V/MgO, which helps to clarify the main features of the process. To do this, several requisites need to be fulfilled: (a) As far as possible, the parameters for each reaction should be obtained from independent experiments, to avoid correlations between parameters of different reactions. (b) Inhibition effects from the reaction products should be investigated, since these may be partly responsible for the discrepancies observed. (c) The qualitative nature of the model proposed should be borne by the experimental data; i.e., if a Mars–van Krevelen mechanism is postulated, a significant availability of lattice oxygen must be demonstrated for the catalyst. (d) The model resulting from the fit of the data obtained in differential reactor experiments with different feed compositions should have predictive capabilities; i.e., it should be able to simulate the reactor performance at integral conversions. This requires a set of experimental data obtained under experimental conditions far removed from those employed to obtain the kinetic model.

2. EXPERIMENTAL

2.1. Catalyst Preparation and Characterization

A V/MgO catalyst with 24 wt% V_2O_5 was prepared following a method similar to that described by Chaar *et al.* (5). MgO powder was impregnated with a solution containing ammonium vanadate (1 wt%) and ammonium hydroxide (0.5 wt%). The resulting suspension was evaporated while stirring until a paste was obtained. This slurry was dried at 120°C, then calcined at 600°C, pelletized, crushed, and sieved to the desired particle size.

The BET surface area was 70 m^2/g. XRD spectra (not shown) indicated a well-crystallized magnesium oxide phase together with a poorly crystallized magnesium orthovanadate. In temperature-programmed-reduction (TPR) runs a broad peak appeared around 300°C and a sharp peak at 675°C.

2.2. Reaction System

The kinetic study was carried out using a 6-mm-internal-diameter tubular quartz reactor inside an electrical furnace. The temperature was measured with a thermocouple inside a quartz thermowell, at the center of the catalyst bed, which contained 20–50 mg of V/MgO catalyst. A PID controller maintained temperature variations within ±0.5°C of the set point. The reactor feed contained oxygen and butane, 1-butene, or butadiene as hydrocarbons, diluted in He. In some experiments aimed at assessing possible inhibition effects H_2O, butadiene, or CO_2 was added to the feed. In the experiments where water was fed, a measured fraction of the gas feed stream was bubbled through a saturator at a controlled temperature. All the streams were mass flow controlled (Brooks). The range of operating conditions was as follows: temperature, 475 to 550°C; total feed flow rate, 200 to 600 ml(STP)/min; oxygen, 2 to 10%; hydrocarbon, 2 to 10%; water, 0 to 3%; CO_2, 0 to 3%; with He as the balance.

As mentioned above, in the differential reactor experiments less than 50 mg of catalyst was used, which resulted in conversion levels always less than 10% and usually smaller than 5%. A larger amount of catalyst, around 200 mg, was employed in the integral reactor experiments used to assess the predictive capability of the kinetic model developed. In this integral reactor, there were several temperature measuring points to detect any temperature inhomogeneities in the bed. The exit gases from both reactors were analyzed online by gas chromatography (HP-5890 Series II) with TCD and FID, using 27% SP-1700 on 80/100 Chromosorb PAW and Molecular Sieve 5A 60/80 columns. This system allowed the separation of butane, 1-butene, *cis*-2-butene, *trans*-2-butene, butadiene, CO, CO_2, and O_2. Carbon mass balance closures were always better than ±5% and usually better than ±3% for the experiments reported in this work.

Varying the hydrocarbon in the feed allowed us to decouple the reactions involved in the network considered. To do this, we proceeded backward in the reaction scheme: the only reactions considered for butadiene were further oxidations to CO and CO_2; it was therefore possible to obtain the kinetic parameters for these reactions independently, feeding butadiene/oxygen mixtures. Butene could give butadiene, CO, and CO_2; therefore, once the kinetics of butadiene oxidation to CO and CO_2 were known, their contributions could be taken into account when considering the reactions of butene, in experiments with a reactor feed containing butene and oxygen. Similarly, these were taken into account for the reactions of butane (to butene, butadiene, CO, and CO_2).

Preliminary experiments varying the particle size of the catalyst and the gas velocity were performed to select the range of operating conditions where mass transfer resistances could be neglected. In addition, experiments without catalyst showed that, under the experimental conditions employed in this study, the gas-phase reaction was not detectable. Prolonged experiments were also carried out to assess the stability of the catalyst. It was found that a significant decrease of activity (ca. 20%) occurred in the first 2 h of operation; then the deactivation rate slowed down, and after about 6 h the catalyst showed stable performance. Therefore kinetic data were obtained after this stabilization time.

Finally, some experiments were also carried out to study the reactivity of lattice oxygen in the V/MgO catalyst. A different experimental system was used, in which pulses of a premixed gas stream were sent over the catalyst by means of a six-way valve. A mass spectrometer (Hyden 2000) was used to analyze the exit gases. Mass-to-charge ratios characteristic of CO, CO_2, butene, and butadiene were continuously monitored. Additionally, the exiting pulses were analyzed by gas chromatography. In the experiments, He (50 ml/min) was employed as a carrier, and pulses (ca. 1 ml) containing 50 vol% butane were sent to a bed of catalyst (40 mg). Before the pulses, the catalyst was exposed to a certain reaction atmosphere for 30 min.

3. EXPERIMENTAL RESULTS

Several sets of experiments were carried out, varying the feed composition, the space time, and temperature.

The effect of the space time on butane conversion and selectivity to the different products for a feed containing butane and oxygen is shown in Figs. 1a and 1b. It can be observed that the selectivity to carbon oxides (Fig. 1a) increases with space time, a behavior characteristic of secondary products. However, extrapolation to zero W/F results in a nonzero selectivity, which implies that CO and CO_2 are also primary products. The selectivity to each of the butenes (Fig. 1b) decreases as the conversion of butane increases, as may be expected for intermediate products. Lastly, it is found that the selectivity to butadiene increases with W/F, but is still significant when W/F approaches zero; again, this indicates that butadiene is both a primary product and a secondary product of the reaction of butane. When the same experiment was repeated using butene/oxygen mixtures the results obtained (Fig. 1c) indicated that butadiene is a primary product of the reaction of butene, while CO and CO_2 are both primary and

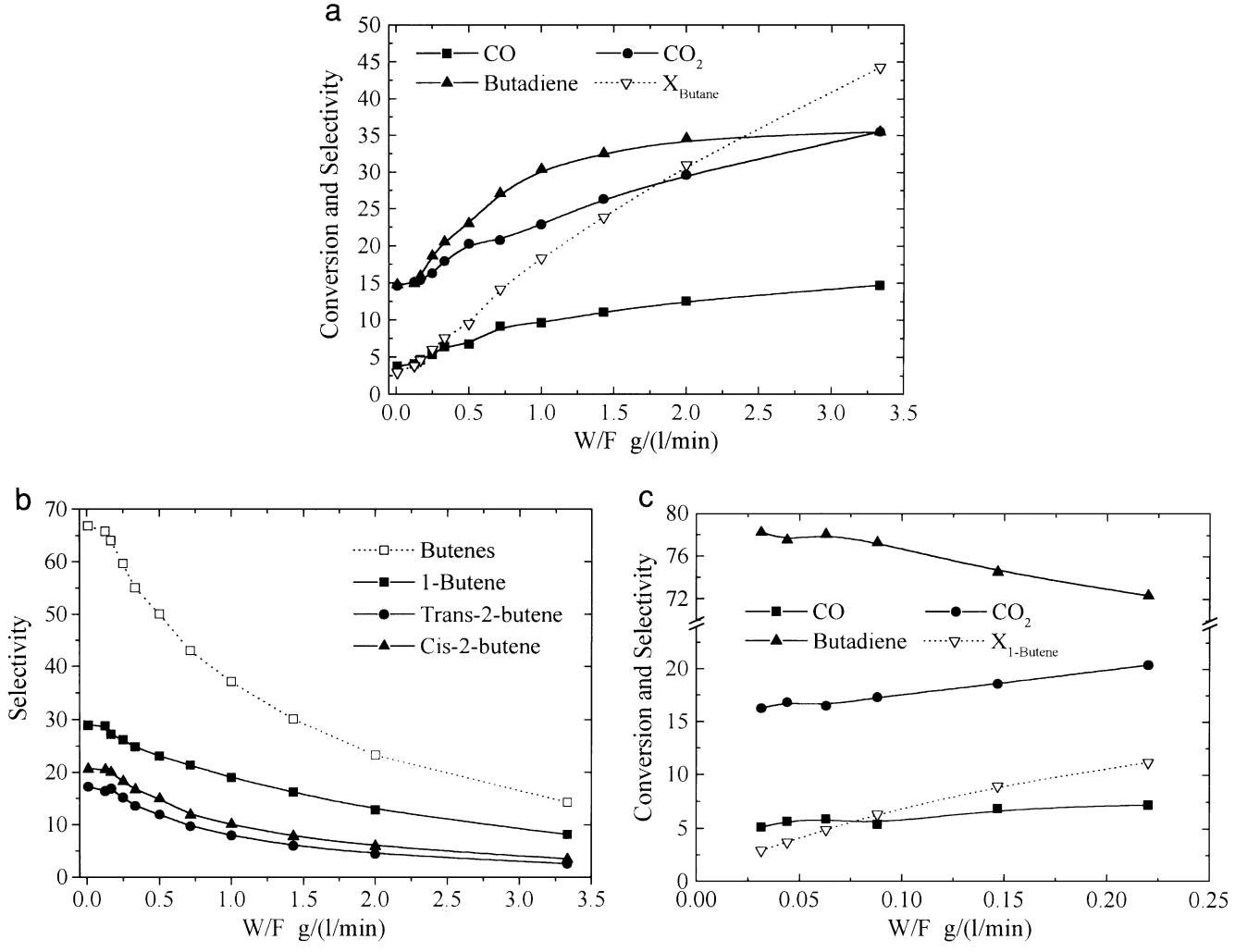

FIG. 1. Variation of hydrocarbon conversion and of the selectivity to each group of products with space time. (a, b) Experiments with butane and oxygen in the feed. (c) Experiments with 1-butene in the feed. Temperature: 500°C; hydrocarbon/oxygen/helium molar ratio: 4/8/88.

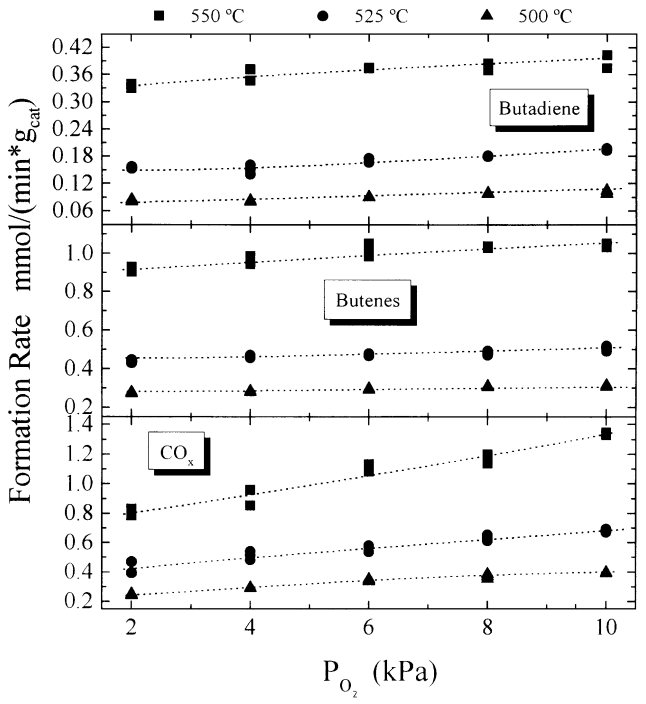

FIG. 2. Effect of the oxygen partial pressure on the rate of formation of CO_x, butenes, and butadiene. Butane and oxygen are present in the feed. Butane partial pressure: 4 kPa; catalyst weight: 50 mg; total flow rate: 300 ml/min.

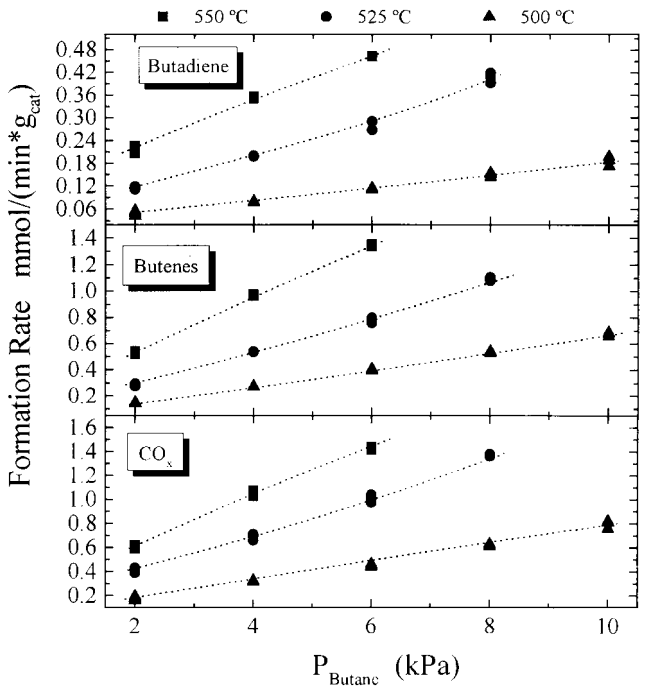

FIG. 3. Effect of butane partial pressure on the rate of formation of CO_x, butenes, and butadiene. Butane and oxygen are present in the feed. Oxygen partial pressure: 8 kPa; catalyst weight: 50 mg; total flow rate: 300 ml/min.

secondary products. All of these results are in agreement with the reacting network given by [1].

Some of the experimental results obtained with feeds containing butane as the hydrocarbon are shown in Figs. 2 and 3. Figure 2 shows the effect of oxygen partial pressure on the CO_x, butene, and butadiene formation rates, while the influence of butane partial pressure is shown in Fig. 3 and the results of equivalent experiments when 1-butene or butadiene was fed are shown in Figs. 4 and 5, respectively. Other series of experiments (not shown) used a constant pressure of butene of butadiene as hydrocarbon in the feed and a variable partial pressure of oxygen. Under differential reaction conditions, each reaction rate was calculated directly from the corresponding product yield. The backward calculation scheme explained above enabled calculation of the net rates for the reactions shown in [1], which would not be possible if only butane and oxygen were fed to the reactor.

Some additional experiments were performed to study potential inhibition effects of the reaction products. Figure 6 shows the effect on the reaction rate of increasing concentrations of water in the feed. A clear inhibition effect is observed, with butane conversion dropping from about 6% to less than 4% when about 2% water was included in the reactor feed. A good fit ($R = 0.99$) of the data obtained with water inhibition is given by the expression

$$r_{iw} = \frac{r_i}{(1 + K_w * P_w)} \qquad [2]$$

where r_{iw} and r_i are the reaction rates in the presence and the absence of water inhibition, respectively. The values of K_w in the temperature interval studied (500–550°C) were constant within ±5%, and the average value of 41.2 atm^{-1} was used in the kinetic model.

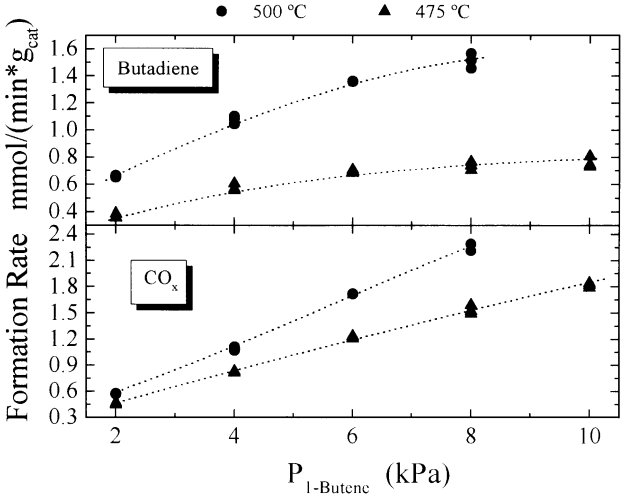

FIG. 4. Effect of 1-butene partial pressure on the rate of formation of CO_x and butadiene. 1-Butene and oxygen are present in the feed. Oxygen partial pressure: 8 kPa; catalyst weight: 22 mg; total flow rate: 250 ml/min.

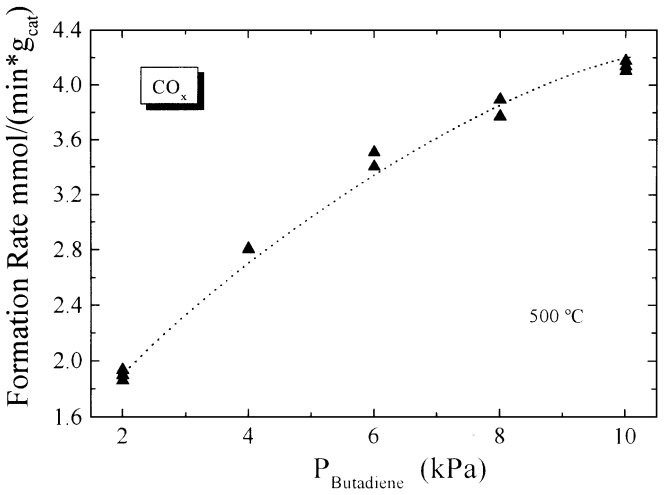

FIG. 5. Effect of butadiene partial pressure on the rate of formation of CO_x. Butadiene and oxygen are present in the feed. Oxygen partial pressure: 8 kPa; temperature: 500°C; catalyst weight: 32.3 mg; total flow rate: 500 ml/min.

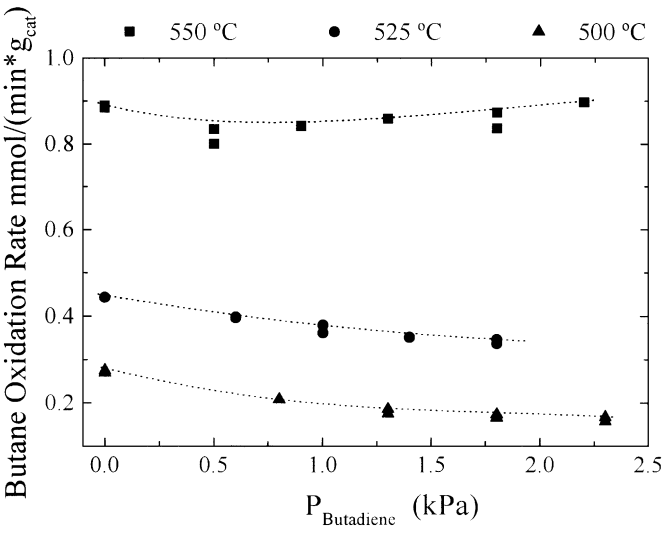

FIG. 7. Effect of butadiene partial pressure on the butane oxidation rate. Butane/oxygen/helium molar ratio: 4/8/88; catalyst weight: 30 mg; total flow rate: 200 ml/min.

Experiments with CO_2 added to the feed (not shown) did not reveal any significant inhibition effect. On the other hand, a clear inhibition effect of butadiene on the butane reaction rate was observed. Figure 7 plots the rate of formation of butene as a function of the concentration of butadiene added to the feed. We chose to plot butene production rather than butane consumption because the former could be determined with higher precision. It can be seen that the inhibition effect decreases as the temperature is increased, which would suggest a competition between butadiene and butane (and probably also butenes) for the same sites on the catalyst surface.

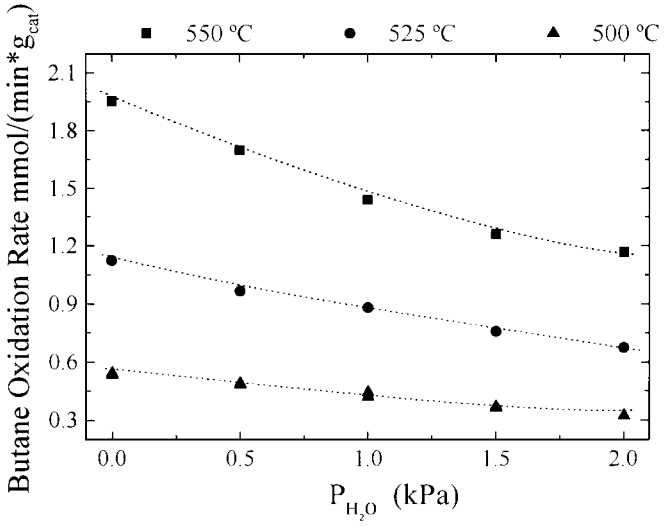

FIG. 6. Effect of water partial pressure on the butane oxidation rate. Butane/oxygen/helium molar ratio: 4/8/88; catalyst weight: 40 mg; total flow rate: 400 ml/min.

Anaerobic experiments. In these experiments, the catalyst was previously equilibrated under the reaction atmosphere resulting from different butane/oxygen ratios in the reactor feed. Butane/He pulses were then introduced, and the reaction products were followed by mass spectrometry. Figure 8 shows the conversion and selectivity obtained with series of 26 butane/He pulses over catalysts equilibrated in the reaction of mixtures with $C_4H_{10}/O_2/He$ ratios of 4/8/88 and 4/2/94, respectively. It seems clear that even the catalyst equilibrated under the most reducing atmosphere employed in these experiments (4/2/94) is able to oxidize butane in the absence of gas-phase oxygen, using oxygen from the lattice. The selectivity to olefins increases with the degree of reduction: the sample that was previously exposed to a more oxidizing atmosphere presents initially a lower selectivity to olefins and a higher production of carbon oxides. As the catalyst is reduced the activity decreases and the selectivity increases for both catalyst samples. These results are taken into account in the kinetic modeling.

4. KINETIC MODELING

The data obtained in the differential reactor were fitted to a power-law model and different mechanistic models. There are several possible choices of mechanistic models. A discussion of the selection procedure is presented next, together with a detailed description of the selected model.

The reaction network considered was a series-parallel network, where CO and CO_2 can be formed from every hydrocarbon; butene can be formed only from butane; and butadiene from both, butane and butene. This reaction network is consistent with the experimental data (selectivity–conversion plots) already discussed.

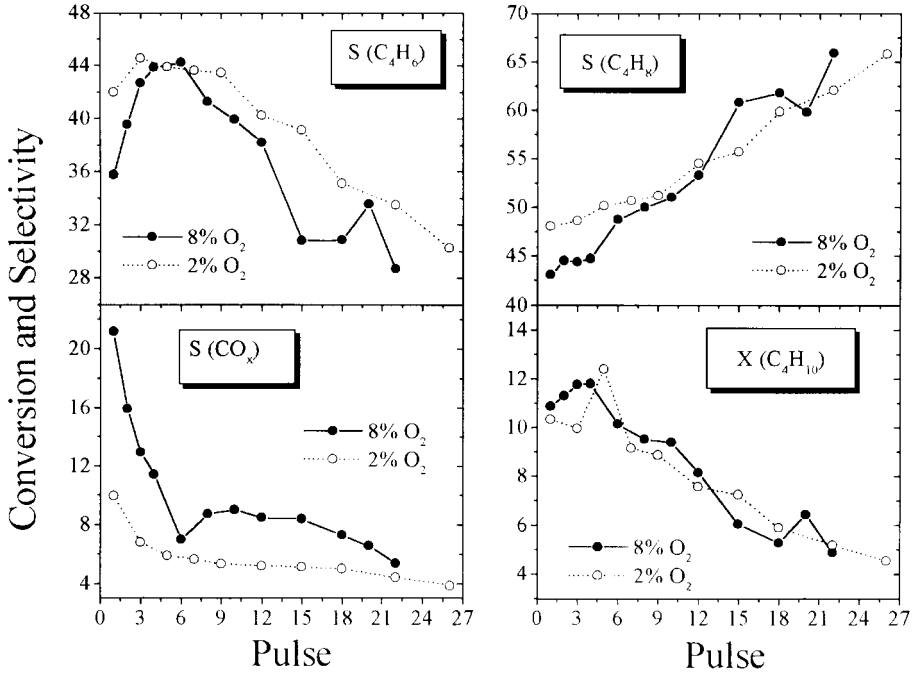

FIG. 8. Butane conversion and selectivity to butenes, butadiene, and CO_x. Anaerobic experiments using butane pulses. Before the pulses, the catalysts was equilibrated under reaction atmospheres containing 8 or 2% oxygen. Butane/oxygen/helium ratio: 4/8/88 or 4/2/94; catalyst weight: 40 mg; total flow rate: 300 ml/min; temperature: 500°C.

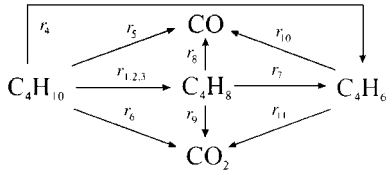

[3]

Reactions 1, 2, and 3 in this scheme refer respectively to the formation of 1-butene, *cis*-2-butene, and *trans*-2-butene from butane.

4.1. Power-Law Model

This model is useful mainly for engineering purposes, as it facilitates comparison of the effects of the different operation variables on the reactions considered. The reaction rates for each of the reactions in the network given by [3] can be written as

$$r_i = k_i * P_{O_2}^n P_{HC}^m, \qquad [4]$$

where P_{HC} represents the partial pressure of the hydrocarbon that disappears in reaction i. The kinetic coefficient is given by

$$k_i = k_{i0} e^{-E_{ai}*(1/T-1/T_0)}, \qquad [5]$$

with T_0 being the reference temperature (773 K).

To obtain the values of the different constants in each of the reaction rate equations, a nonlinear fit of the data obtained in the differential reactor was carried out. In this case, the kinetic parameters for the reactions where butane disappears (reactions 1 to 6 in the above network) were obtained directly from experiments with butane and oxygen in the feed, while those for reactions 7 to 9 and 10 and 11 were obtained from the results of experiments with feeds containing butene and oxygen and butadiene and oxygen, respectively. While the kinetic model considers the formation of each of the butene isomers independently, we do not have enough data to calculate the rate of consumption of each of the isomers independently. A rough estimation can be obtained from the analysis of the data in Fig. 1B, which shows that *cis*- and *trans*-2-butene disappear at a higher rate (ca. 1.7 times faster) than *n*-butene as the space time is increased.

The parameters obtained from data fitting using the commercial software Scientist are shown in Table 1. Despite its simplicity, the power-law model lays out some of the main trends in the reaction considered. Thus, it may be noted in Table 1 that the reaction order with respect to oxygen for the formation of butenes and butadiene from butane is considerably smaller than that for the formation of CO_x. This suggests that a reactor that keeps a low partial pressure of oxygen would give a higher selectivity to olefins, as has been found experimentally using a porous membrane to distribute oxygen to a fixed bed of V/MgO catalyst (8).

TABLE 1

Kinetic Parameters Obtained by a Power-Law Fit of Differential Reactor Data

Reaction[a]	k [mmol/(min $*$ g $*$ atm^{n+m})]	E_a (kJ/mol)	n	m	R
1	4.59 ± 0.34	146.5 ± 2.6	0.10 ± 0.01	1.04 ± 0.03	0.997
2	2.17 ± 0.16	142.1 ± 2.5	0.09 ± 0.01	1.01 ± 0.03	0.997
3	2.38 ± 0.15	136.7 ± 2.1	0.08 ± 0.01	1.10 ± 0.02	0.998
4	3.00 ± 0.31	162.3 ± 3.6	0.12 ± 0.02	1.00 ± 0.04	0.995
5	1.61 ± 0.27	168.7 ± 5.7	0.28 ± 0.04	1.12 ± 0.06	0.988
6	3.14 ± 0.28	121.5 ± 2.9	0.33 ± 0.02	0.93 ± 0.03	0.996
7	24.3 ± 4.00	181.6 ± 4.5	0.34 ± 0.03	0.67 ± 0.04	0.993
8	5.08 ± 2.37	160.5 ± 1.3	0.35 ± 0.08	1.03 ± 0.12	0.940
9	15.9 ± 1.95	118.5 ± 3.5	0.28 ± 0.02	1.05 ± 0.03	0.995
10	1.93 ± 0.31	178.8 ± 5.2	0.65 ± 0.04	0.25 ± 0.04	0.994
11	9.97 ± 5.10	143.0 ± 20	0.50 ± 0.02	0.50 ± 0.01	0.999

[a] Reaction number refers to numbers in Eq. [3].

Also, the apparent activation energy is higher for butadiene and CO formation from butane than for CO_2 formation from butane, while the activation energy for the formation of butenes has an intermediate value. This means that the selectivity to butadiene and the CO/CO_2 ratio would be expected to increase with temperature. Also, since the CO formation rate from butane is considerably smaller than the CO_2 formation rate, the total selectivity to olefins is also expected to increase with temperature. All of these predictions agree with the experimental results.

Regarding the products obtained from butene, the reaction order with respect to oxygen given in Table 1 for CO_x formation is similar or even slightly smaller than the values corresponding to butadiene formation. Therefore there is no favorable kinetic effect for oxygen distribution, and it may be expected that decreasing the oxygen concentration will not result in an improvement of the selectivity to butadiene. Finally, comparison of the reactions of butene and butane shows that the effect of temperature is analogous (similar apparent activation energies), although butene is more reactive than butane, the reaction rate being three to five times that of butane under similar conditions.

4.2. Mechanistic Models

Kinetic equations obtained from mechanistic consideration offer several advantages over power-law kinetics, since they provide information about the reaction mechanism and can often be extrapolated to conditions outside the range of experimental data used to obtain them. As a first step, several mechanisms have been considered for the study of the reactions of butane oxidation (to butenes, CO_x, and butadiene):

(a) Mars–van Krevelen, where the catalyst operates in redox cycles, being reduced by the hydrocarbon and oxidized by gaseous oxygen;

(b) Langmuir–Hinshelwood, where adsorbed butane reacts with adsorbed oxygen, and both are adsorbed in different sites (noncompetitive adsorption);

(c) Eley–Rideal, where the rate-determining step is the reaction between an adsorbed species and another species in the gas phase, e.g., oxygen in the gas phase with adsorbed butane.

Only the experiments with butane in the feed were fit in this stage. Since the butane conversion was small, the effect of other hydrocarbons on the reaction rate was neglected in this first approach.

The equations corresponding to each of the above mechanisms are shown in Table 2, where $n = 1$ corresponds to models in which nondissociative oxygen adsorption takes place, and $n = 0.5$ to dissociative oxygen adsorption. Although the fitting obtained with the Langmuir–Hinshelwood or Eley–Rideal model was acceptable, many of the kinetic parameters obtained had out-of-range values. On the other hand, the standard errors obtained using these models were often higher than the value of the parameter sought, sometimes by several orders of magnitude. These results showed the inadequacy of the Langmuir–Hinshelwood or Eley–Rideal model for the process studied. On the other hand, our experimental observations indicated that the catalyst had a significant redox capability, being able to oxidize butane in the absence of gas-phase oxygen. Therefore, we chose to carry out a deeper study of the Mars–van Krevelen model using several variants of the mechanism, described next. The reaction rate equations are shown in Table 3.

M1. A model with a single type of active site (θ_O): It has been assumed that the reaction rate for site reoxidation is proportional to the oxygen partial pressure. Two possibilities are considered:

M1a. A reaction order of 1 (a in Table 3) with respect to the concentration of oxidized (active) sites, for both selective and nonselective reactions.

M1b. A reaction order of 1 with respect to the concentration of oxidized sites for the selective reactions and of 2

TABLE 2

Reaction Rate Equations Employed to Fit the Data on Butane Oxidation (to Butenes, Butadiene, and CO_x)

Model	Expression
Mars–van Krevelen model	$r_i = \dfrac{k_{iox} * P_{O_2}^n * k_{ired} P_{C_4H_{10}}}{k_{iox} * P_{O_2}^n + k_{ired} P_{C_4H_{10}}}$
Langmuir–Hinshelwood model Noncompetitive adsorption	$r_i = \dfrac{k_{reac} * K_{O_2}^n * P_{O_2}^n * K_{C_4H_{10}} P_{C_4H_{10}}}{(1 + K_{O_2}^n * P_{O_2}^n) * (1 + K_{C_4H_{10}} * P_{C_4H_{10}})}$
Eley–Rideal model	$r_i = \dfrac{k_{reac} * K_{O_2} * P_{O_2}^n * P_{C_4H_{10}}}{(1 + K_{O_2} * P_{O_2}^n + K_{C_4H_{10}} * P_{C_4H_{10}})}$

TABLE 3

Reactions That Constitute the Mars–van Krevelen Models Discussed and Corresponding Reaction Rate Equations

Model	Rate expression	Reaction (in Eq. [3])
M1	$r_i = k_i * P_{HC} * \theta_O^a$ $r_{OX1} = k_{OX1} * P_{O_2} * (1-\theta_O)$	$i = 1$–11
M2	$r_i = k_i * P_{HC} * \theta_O$ $r_i = k_i * P_{HC} * \lambda_O$ $r_{OX1} = k_{OX,\theta} * P_{O_2}^{n_1} * (1-\theta_O)$ $r_{OX2} = k_{OX,\lambda} * P_{O_2}^{n_2} * (1-\lambda_O)$	$i = 1$–4, 7 $i = 5, 6, 8$–11
M3	$r_i = k_i * P_{HC} * \theta_O$ $r_i = k_i * P_{HC} * \theta_{OO}$ $r_{OX1} = k_{OX,\theta_O} * P_{O_2}^{0.5} * (1-\theta_O-\theta_{OO})$ $r_{OX2} = k_{OX,\theta_{OO}} * P_{O_2}^{0.5} * \theta_O$	$i = 1$–4, 7 $i = 5, 6, 8$–11
M4	$r_i = k_i * P_{HC} * \theta_O$ $r_i = k_i * P_{HC} * \lambda_O$ $r_{OX1} = k_{OX,\theta} * P_{O_2}^{0.5} * (1-\theta_O)$ $r_{OX2} = k_{OX,\lambda} * P_{O_2}^{1} * (1-\lambda_O)$	$i = 1$–11 $i = 5, 6, 8$–11

(a in Table 3) for the nonselective reactions (CO and CO_2 formation).

M2. A model with two different types of active sites: In the first type (θ_O) the selective reactions occur, while on the second type (λ_O) only carbon oxides are produced. The reaction order with respect to the concentration of each type of active site is 1. Several possible alternatives are considered:

M2a. The reaction order with respect to oxygen for the reoxidation of selective and nonselective sites (n_1 and n_2 in Table 3) is taken equal to 0.5 and 1, respectively.

M2b. The above indicated reaction orders are taken equal to 1 in both cases.

M2c. The reaction order with respect to oxygen for the reoxidation of selective and nonselective sites (n_1 and n_2 in Table 3) is taken equal to 1 and 2, respectively.

M3. A model with two types of active sites (selective, θ_O, and nonselective, θ_{OO}) that can be interconverted, as postulated by Mamedov and Cortés-Corberán (2). In this case the reaction order with respect to oxygen is taken as 0.5 in the reoxidation of selective sites and 1 in nonselective sites.

M4. Model with two types of active sites, I (θ_O) and II (λ_O): On type I sites both selective and nonselective reactions occur, while on sites II only nonselective reactions take place, as proposed by Pantazidis (19). The reaction order with respect to the concentration of oxidized sites is taken as 1 in both cases, while the reaction order with respect to oxygen is 0.5 for sites I and 1 for sites II.

The operating algorithm followed to determine the kinetics of competing mechanisms was as follows: In a first step, the results of experiments with butadiene and oxygen in the feed are used to obtain the kinetics of butadiene oxidation (which for the model finally selected correspond to the kinetic coefficients k_{10} and k_{11}; see Table 7 below). These kinetic parameters are considered fixed, which allows us to take butadiene oxidation into account to calculate the kinetics of the reactions of butene to yield butadiene, CO, and CO_2 (k_7 to k_9). In a similar way, the kinetics for the reactions of butane (k_1 to k_6) are calculated taking into account the already known coefficients (k_7 to k_{11}).

Once the kinetics have been calculated in a stepwise mode, the adequacy of the models in representing the kinetic data can be assessed. Table 4 lists the best-fit regression coefficient and model selection criterion (MSC) for each of the above-described models. The MSC is computed as

$$\mathrm{MSC} = \ln\left[\frac{\sum_{j=1}^{l}\left(Y_{\mathrm{obs}_j} - \bar{Y}_{\mathrm{obs}}\right)^2}{\sum_{j=1}^{l}\left(Y_{\mathrm{obs}_j} - Y_{\mathrm{cal}_j}\right)^2}\right] - \frac{2p}{j}, \qquad [6]$$

where j is the number of experimental points, p is the number of parameters, and $\bar{Y}_{\mathrm{obs}}$ is the weighted mean of the experimental observations.

The MSC is useful because it takes into account the number of parameters of a given mode, and therefore allows comparison of different models. Among the models described above, the best fit is given by models M4 and M2b, with MSC values of 3.996 and 3.849, respectively. A closer comparison of both models is made in Tables 5 and 6, respectively. In Table 5 it can be seen that some of the parameters for model M4 (those concerning reactions over type II sites) are incongruent. As a consequence, model M2b is selected; i.e., it is considered that the catalyst surface has selective and nonselective active sites that cannot be interconverted. Further, the different reactions are assumed to follow a first-order dependency with respect to the concentration of the corresponding type of sites, and the rate of reoxidation is directly proportional to the oxygen partial pressure. The considered reactions and their rate expressions are given in Table 7.

Obviously, the reactions given in Table 7 are not elementary steps, but the proposed reaction rate equation can be

TABLE 4

Comparison of the Different Mars–van Krevelen Models with Respect to Goodness-of-Fit

Model	R	MSC
M1a	0.9916	3.652
M1b	0.9930	3.830
M2a	0.9929	3.802
M2b	0.9932	3.849
M2c	0.9928	3.795
M3	0.9921	3.703
M4	0.9942	3.996

TABLE 5

Kinetic Parameters of Model M4

Reaction	k_{0i} (mmol/min ∗ g)	E_{ai} (kJ/mol)	Reaction	k_{0i} (mmol/min ∗ g)	E_{ai} (kJ/mol)
1	3.689 ± 0.127	132.5 ± 9.6	5	1.45 ± 0.49	137.5 ± 42.6
2	1.940 ± 0.092	130.0 ± 9.6	6	3.62 ± 0.53	91.5 ± 21.8
3	2.349 ± 0.100	126.6 ± 9.1	12	93.5 ± 19.2	152.6 ± 48.8
4	2.512 ± 0.120	149.6 ± 85	13	134.2 ± 35.0	181.9 ± 55.4
5′	$8.16E5 \pm 10.3E9$	$37.5 \pm 6.30E8$			
6′	$27.2E5 \pm 34.4E9$	$6.7 \pm 6.30E8$			

Note. Reactions 1–6 denote butane oxidation to 1-butene, *trans*-2-butene, *cis*-2-butene, butadiene, CO, and CO_2, in this order, when occurring on type I sites; reactions 5′ and 6′ denote, respectively, butane oxidation to CO and CO_2 when occurring on type II sites; and reactions 12 and 13 denote catalyst oxidation.

TABLE 6

Kinetic Parameters of Model M2b

Reaction	k_{0i} (mmol/min ∗ g)	E_{ai} (kJ/mol)	Reaction	k_{0i} (mmol/min ∗ g)	E_{ai} (kJ/mol)
1	3.74 ± 0.15	144.9 ± 5.1	8	1.94 ± 0.09	146.2 ± 14.5
2	1.97 ± 0.10	142.7 ± 6.8	9	6.94 ± 0.19	107.2 ± 7.7
3	2.38 ± 0.11	139.1 ± 6.0	10	7.09 ± 0.23	146.6 ± 9.6
4	1.85 ± 0.11	148.5 ± 8.1	11	26.1 ± 1.47	102.0 ± 8.0
5	0.55 ± 0.03	175.5 ± 6.2	12	179.7 ± 96.1	114.5 ± 65.8
6	1.55 ± 0.05	138.4 ± 4.4	13	195.3 ± 32.6	5.5 ± 19.4
7	41.1 ± 1.1	164.7 ± 10.9			

Note. Reactions in Table 7.

TABLE 7

Elementary Reactions Considered in Model M2b

Reaction	Rate expression	Equation
Butane oxidation		
$C_4H_{10} + X_O \rightarrow 1 - C_4H_8 + H_2O + X$	$r_1 = k_1 * P_{C_4H_{10}} * \theta_O$	[7]
$C_4H_{10} + X_O \rightarrow trans - 2 - C_4H_8 + H_2O + X$	$r_2 = k_2 * P_{C_4H_{10}} * \theta_O$	[8]
$C_4H_{10} + X_O \rightarrow cis - 2 - C_4H_8 + H_2O + X$	$r_3 = k_3 * P_{C_4H_{10}} * \theta_O$	[9]
$C_4H_{10} + 2X_O \rightarrow C_4H_6 + H_2O + 2X$	$r_4 = k_4 * P_{C_4H_{10}} * \theta_O$	[10]
$C_4H_{10} + 9Z_O \rightarrow 4CO + 5H_2O + 9Z$	$r_5 = k_5 * P_{C_4H_{10}} * \lambda_O$	[11]
$C_4H_{10} + 13Z_O \rightarrow 4CO_2 + 5H_2O + 13Z$	$r_6 = k_6 * P_{C_4H_{10}} * \lambda_O$	[12]
Butene oxidation		
$C_4H_8 + X_O \rightarrow C_4H_6 + H_2O + X$	$r_7 = k_7 * P_{C_4H_8} * \theta_O$	[13]
$C_4H_8 + 8Z_O \rightarrow 4CO + 4H_2O + 8Z$	$r_8 = k_8 * P_{C_4H_8} * \lambda_O$	[14]
$C_4H_8 + 12Z_O \rightarrow 4CO_2 + 4H_2O + 12Z$	$r_9 = k_9 * P_{C_4H_8} * \lambda_O$	[15]
Butadiene oxidation		
$C_4H_6 + 7Z_O \rightarrow 4CO + 3H_2O + 7Z$	$r_{10} = k_{10} * P_{C_4H_6} * \lambda_O$	[16]
$C_4H_6 + 11Z_O \rightarrow 4CO_2 + 3H_2O + 11Z$	$r_{11} = k_{11} * P_{C_4H_6} * \lambda_O$	[17]
Catalyst oxidation		
$O_2 + 2X \rightarrow 2 * X_O$	$r_{12} = k_{12} * P_{O_2} * \theta$	[18]
$O_2 + 2Z \rightarrow 2 * Z_O$	$r_{13} = k_{13} * P_{O_2} * \lambda$	[19]

Note. The kinetic coefficients are given by Eq. [5].

easily explained as series of elementary steps, with one of them being the rate-determining step. For example, Eq. [10] can be considered as the combination of the following elementary steps:

$$C_4H_{10} + X\text{–}O \xrightarrow{k} C_4H_9 + X\text{–}OH, \quad \text{rate-determining step,} \quad [20]$$

$$C_4H_9 + X\text{–}OH \rightarrow X\text{–}OH_2 + C_4H_8, \quad \text{fast step,} \quad [21]$$

$$C_4H_8 + X\text{–}O \rightarrow C_4H_7 + X\text{–}OH, \quad \text{fast step,} \quad [22]$$

$$C_4H_7 + X\text{–}OH \rightarrow X\text{–}OH_2 + C_4H_6, \quad \text{fast step,} \quad [23]$$

$$X\text{–}OH_2 \leftrightarrow X + H_2O, \quad \text{equilibrium.} \quad [24]$$

We wish to attach no particular significance to the details of the above sequence. The steps simply represent the activation of gas-phase hydrocarbon by an oxidized active site, followed by a sequence of fast steps, giving the reaction product and one or more reduced sites.

A pseudo-steady state may be assumed for the degree of oxidation of the catalyst sites, θ_O and λ_O. In this case, the oxidation and the reduction reaction rates should be equal, i.e.,

$$2r_{12} = (r_1 + r_2 + r_3 + 2r_4 + r_7), \quad [25]$$

$$2r_{13} = 9r_5 + 13r_6 + 8r_8 + 12r_9 + 7r_{10} + 11r_{11}. \quad [26]$$

The following equations, describing the dependency of θ_O and λ_O on the operating conditions, can be easily obtained:

$$\theta_O = \frac{k_{12}P_{O_2}}{k_{12}P_{O_2} + (k_1 + k_2 + k_3 + 2k_4) * P_{C_4H_{10}} + k_7 * P_{C_4H_8}}, \quad [27]$$

$$\lambda_O = \frac{k_{13}P_{O_2}}{k_{13}P_{O_2} + (9k_5 + 13k_6) * P_{C_4H_{10}} + (8k_8 + 12k_9) * P_{C_4H_8} + (7k_{10} + 11k_{11}) * P_{C_4H_6}}. \quad [28]$$

These expressions, together with the values given in Table 6, can then be used to calculate the reaction rates in Eq. [7] to [19]. All the reactions rates are corrected by the effect of water, according to Eq. [2]. From the above equations it is also clear that the simultaneous presence of different hydrocarbons reduces the fraction of available active (i.e.,oxidized) sites. This results in a smaller reaction rate of the individual hydrocarbons in the presence of others.

5. COMPARISON OF PREDICTED AND EXPERIMENTAL RESULTS

As stated in the Introduction, one of the requirements for the kinetic model developed in this work was that it should be able to predict reasonably well the reactor performance at integral conversion levels, i.e., under conditions significantly different from those used in the differential

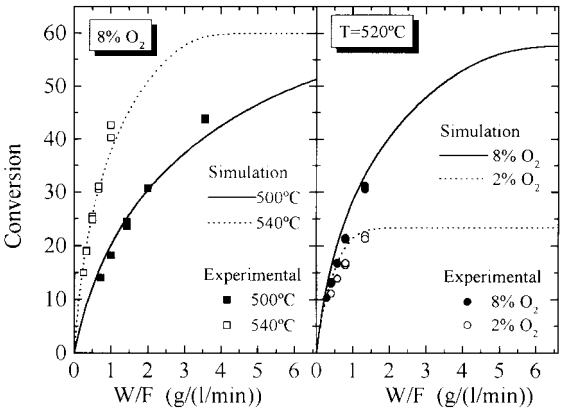

FIG. 9. Comparison of experimental and simulated results. Conversion versus *W/F*. Catalyst weight: 100–250 mg; total flow rate: 75–400 ml/min; butane partial pressure: 4 kPa.

experiments used to obtain the kinetics. To this end, a new series of experiments was carried out in an integral reactor, using different temperatures and feed compositions. The results have been compared with the simulation of a plug-flow fixed-bed reactor using the kinetics given in Table 7. Since no specific reaction data were available for butene isomers, it has been assumed in this simulation that the reaction rates for 2-butenes follow the same expression that has been found for 1-butene, although in agreement with the previous discussion a value 1.7 times higher has been taken for the kinetic constants (preexponential factor) of *cis*- and *trans*-2-butene.

The comparison between theoretical and experimental results is shown in Figs. 9 to 11. It may be seen that the model predicts satisfactorily most of the experimental results, even at conversions as high as 40%:

—the butane conversion for a given spatial time, and its change with the temperature and oxygen concentration (Fig. 9);

—the increase in the selectivity to butadiene and total dehydrogenation products with temperature for a given butane conversion and the shape of the butadiene selectivity-versus-butane conversion curves (Fig. 10);

—the changes in the selectivity to butadiene and total olefins with the oxygen concentration in the feed (Fig. 11).

In general, the simulation of the reactor employing the kinetics corresponding to model M2b predicts well the observed changes in the performance of the reactor. It must be emphasized that no further adjustable parameters are introduced: the model uses the kinetics determined under differential conditions to predict the reactor performance at conversions up to about 40%. In a separate investigation (20), it was also found that the model presented here is useful in predicting reactor performance in a very different system, a membrane reactor.

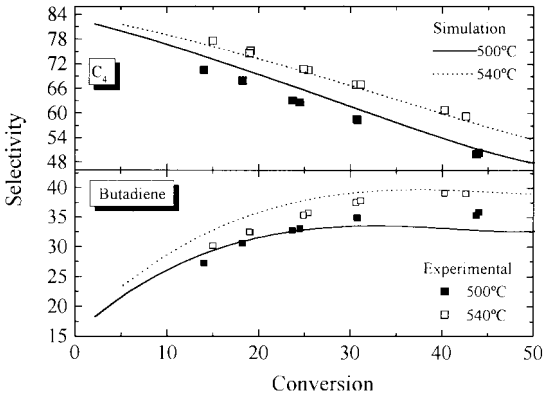

FIG. 10. Comparison of experimental and simulated results. Butadiene and total C_4 (butadiene + butenes) selectivity at two different temperatures: Catalyst weight: 100–250 mg; total flow rate: 75-400 ml/min; butane/oxygen/helium ratio: 4/8/88.

Also, the main features of this model agree with most of the previous findings in the literature. The effect of water as an inhibitor of the reaction rate was also found by Oyama *et al.* (21) and Lemonidou *et al.* (22) in similar systems. As shown in the Introduction, many authors proposed the Mars–van Krevelen mechanism for oxidative dehydrogenation of alkanes on VO_x-supported catalysts, and often different paths for the selective and nonselective reactions have also been proposed (2, 13, 15, 16, 18, 19).

6. CONCLUSIONS

A kinetic model for the process of oxidative dehydrogenation of butane over a V/MgO catalyst has been developed. Extensive experimental work was performed to obtain the kinetic parameters of each reaction involved in the network. A Mars–van Krevelen model with two types of active sites, selective (leading to dehydrogenation products) and nonselective (leading to deep oxidation), provides the best fit. This model explains well the qualitative and quantitative observations presented in this work. Also, a reactor model that employs the kinetic parameters obtained from differential reactor experiments predicted satisfactorily the reactor performance at integral conversion levels.

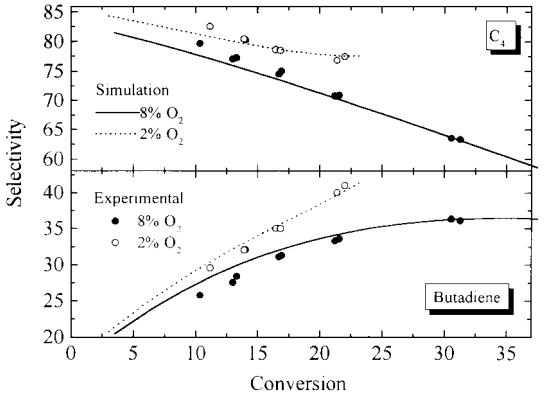

FIG. 11. Comparison of experimental and simulated results. Butadiene and total C_4 (butadiene + butenes) selectivity at two different oxygen partial pressures. Catalyst weight: 100 mg; temperature: 520°C; total flow rate: 75–400 ml/min; butane partial pressure: 4 kPa.

APPENDIX: NOMENCLATURE

E_a	activation energy (kJ/mol)
j	number of experimental points
k	kinetic constant [mmol/(min g atm^{n+m})]
K	equilibrium constant(bar^{-1})
MSC	model selection criterion
n, m	reaction orders in a power-law kinetic equation
p	number of parameters of model
P	partial pressure (bar)
r	reaction rate
T_0	reference temperature
W/F	spatial time (g min/1)
X, Z	reduced active sites
X_O, Z_O	oxidized active sites
Y	value of a specific data point
θ, λ	reduced active site concentration (%1)
θ_O, λ_O	oxidized active site concentration (%1)
θ_{OO}	superoxidized active site concentration (%1)

Subscripts

cal	calculated
i	reaction i
j	experimental points
obs	observed
ox	oxidation (of active sites)
w	water

REFERENCES

1. Kung, H. H., *Adv. Catal.* **40**, 1 (1994).
2. Mamedov, E. A., and Cortés-Corberán, V., *Appl. Catal.* **127**, 1 (1995).
3. Cavani, F., and Trifiró, F., *Catal. R. Soc. Chem.* **11**, 246 (1994).
4. Vrieland, G. E., and Murchison, C. B., *Appl. Catal.* **134**, 101 (1996).
5. Chaar, M. A., Patel, D., and Kung, H. H., *J. Catal.* **109**, 483 (1987).
6. Bhattacharyya, D., Bej, S. K., and Rao, M. S., *Appl. Catal.* **87**, 29 (1992).
7. Blasco, T., López-Nieto, J. M., Dejoz, A., and Vazquez, M. I., *J. Catal.* **157**, 271 (1995).
8. Téllez, C., Menéndez, M., and Santamaría, J., *AIChE J.* **43**, 777 (1977).
9. Soler, J., López-Nieto, J. M., Herguido, J., Menéndez, M., and Santamaría, J., *Catal. Lett.* **50**, 25 (1998).
10. Patel, D., Kung, M. C., and Kung, H. H., *in* "Proceedings, 9th International Congress on Catalysis, Calgary, 1988" (M. J. Phillips and M. Ternan, Eds.), Vol. 4, p. 1554. Chem. Institute of Canada, Ottawa, 1988.
11. Panteleeva, Y. A., Musaev, A. M., Talyshinskii, R. M., Seifullaeva, Zh. M., and Rizaev, R. G., *Kinet. Catal.* **32**, 571 (1991).

12. Madeira, L. M., Maldonado-Hodar, F. J., Portela, M. F., Freire, F., Martin-Aranda, R. M., and Oliveira, M., *Appl. Catal.* **135**, 137 (1996).
13. Dejoz, A., López-Nieto, J. M., Melo, F., and Vazquez, I., *Ind. Eng. Chem. Res.* **36**, 2588 (1997).
14. Anderson, L. S. T., *Appl. Catal.* **112**, 209 (1994).
15. Michaels, J. N., Stern, D. L., and Grasselli., R. K., *Catal. Lett.* **42**, 139 (1996).
16. Stern, D. L., and Graselli, R. K., *J. Catal.* **167**, 560 (1977).
17. Creaser, D., and Anderson, B., *Appl. Catal.* **141**, 131 (1996).
18. Boisdron, N., Monnier, A., Jalowleckl-Duhamel, L., and Barbaux, Y., *J. Chem. Soc. Faraday Trans.* **91**, 2899 (1995).
19. Pantazidis, A., Ph.D. thesis, Lyon, 1996.
20. Téllez, C., Menéndez, M., and Santamaría, J., *in* "Proceedings, 15th ISCRE, Newport Beach, California, 1998," p. 149.
21. Oyama, S. T., Middlebrook, A. M., and Somorjai, G. A., *J. Phys. Chem.* **94**, 5029 (1990).
22. Lemonidou, A. A., Tjatjopoulos, G. J., and Vasalos, I. A., *Catal. Today* **45**, 65 (1998).